

EUROPEAN ORGANIZATION FOR NUCLEAR RESEARCH

CERN-PPE/93-05

11.01.1993

STUDY OF CHARGED PARTICLES EMITTED IN THE β -DECAY OF ${}^{6,8}\text{He}$

M.J.G. Borge^{1,2}, L. Johannsen³, B. Jonson⁴, T. Nilsson⁴, G. Nyman⁴,

K. Riisager³, O. Tengblad², K. Wilhelmsen Rolander⁴

and the ISOLDE Collaboration

KEYWORDS:

RADIOACTIVITY ${}^6\text{He}$ (β^-): measured β -delayed deuteron spectrum, branching ratio deduced.

${}^8\text{He}$ (β^-): measured β -delayed triton and alpha spectra, triton branching ratio deduced.

R-matrix analysis. Energy level in ${}^8\text{Li}$ deduced.

[ThC-C + p] reaction, separation on-line, ΔE -E telescope low energy loss.

Abstract

The beta delayed charged particle spectra from ${}^6\text{He}$ and ${}^8\text{He}$ were measured with a telescope consisting of a gas counter and a Si surface barrier detector. Beta delayed deuterons and tritons are emitted in the two cases with branching ratios of $(7.6 \pm 0.6) \cdot 10^{-6}$, $E_d > 350$ keV, and $(8.0 \pm 0.5) \cdot 10^{-3}$, respectively. Both spectra present anomalies that must be due to the special structure of these nuclei (an alpha core surrounded by several neutrons).

(IS210)

Submitted for publication in Nuclear Physics A

-
1. Insto. Estructura de la Materia, CSIC, Serrano 119, E-28006-Madrid
 2. ISOLDE PPE, CERN, CH-1211-Genève-23
 3. Institut for Fysik og Astronomi, Aarhus Universitet, DK-8000 Aarhus C
 4. Fysiska Institutionen, Chalmers Tekniska Högskola, S-41296 Göteborg

1. Introduction

The anomalously large matter radii of ${}^6\text{He}$, ${}^8\text{He}$ and ${}^{11}\text{Li}$ were discovered in 1985 in reaction experiments [1] with 790 MeV/u beams of radioactive nuclei on low-mass targets. Since then many experiments at different facilities all over the world (see ref. 2 and references therein) have been dedicated to the study of similar nuclei, mainly ${}^{11}\text{Li}$. The results can be interpreted in terms of formation of a neutron halo for those drip-line nuclei that have low enough binding energy for the last neutron(s).

Our aim in this paper is to investigate whether this halo structure would manifest itself in beta decay processes. In a neutron halo nucleus the last neutron, or the last two neutrons (which are most likely in an ${}^1\text{S}$ state), spend a large fraction of their time far away from the core. One could therefore imagine that beta decays take place directly into continuum states with transition probabilities corresponding to a superallowed beta-decay. For a two-neutron halo it is advantageous to let the neutron pair decay into a deuteron due to the gain in energy; this decay mode is energetically possible for both ${}^6\text{He}$ and ${}^8\text{He}$.

The beta-delayed deuteron emission was detected a few years ago in the decay of ${}^6\text{He}$ [3], but the branching ratio obtained was very low and has not yet been fully explained theoretically. The resulting deuteron and alpha (the daughter nucleus) spectra are characterized by a continuous distribution peaking at low energies, but the two distributions were not resolved from one another. In order to distinguish between these particles we had to develop a detector capable of identifying low energy charged particles of different charges. For this purpose a ΔE - E telescope with low energy loss was constructed; a detailed description is given below.

It is not known whether ${}^8\text{He}$ has a neutron halo (the neutron separation energy is not very low). We decided nevertheless to make use of the telescope to remeasure the beta-delayed triton branch in ${}^8\text{He}$. An exhaustive study of the beta decay of this nucleus has been made by Barker and Warbuton [4] in terms of multi-level, multi-channel R-matrix theory. The values of the R-matrix were adjusted to best fit the data. The resulting

reduced width amplitudes for the ${}^8\text{Li}^*$ levels are in good agreement with shell-model calculations [5] except for the triton branch where the reduced width was underestimated by a factor of three. We have analyzed our new triton data within the R-matrix formalism to clarify this point.

2. Experimental Set-up

The nuclei ${}^6\text{He}$ ($2 \cdot 10^5$ ions/s) and ${}^8\text{He}$ ($2.3 \cdot 10^4$ ions/s) were produced in nuclear reactions induced by a 910 MeV $1 \mu\text{A}$ ${}^3\text{He}$ beam from the CERN Synchro-cyclotron impinging on a ThC-C target and ionized by a direct heated FEBIAD ion-source filled with Ar. After this, the ion beam was accelerated to 60 keV, mass separated at ISOLDE 2 and stopped in a $100 \mu\text{g}/\text{cm}^2$ C-foil. The foil was tilted with respect to the beam so that the effective thickness was increased by 23%.

The Monte Carlo computer code TRIM [6] was used to calculate the slowing down and scattering of the 60 keV ions in the C-foil. A mean range of $86 \mu\text{g}/\text{cm}^2$ was calculated for the ${}^6\text{He}$ ions with FWHM longitudinal and lateral straggling of $11 \mu\text{g}/\text{cm}^2$ and $16 \mu\text{g}/\text{cm}^2$, respectively. The corresponding values for the ${}^8\text{He}$ ions are a mean range of $91.5 \mu\text{g}/\text{cm}^2$ and a FWHM longitudinal and lateral straggling of $15.5 \mu\text{g}/\text{cm}^2$ and $18 \mu\text{g}/\text{cm}^2$, respectively. The calculation thus shows that essentially all the ions are stopped in the foil.

The C-foil was mounted on a wheel which had, at its opposite side, a ${}^{148}\text{Gd}$ alpha-source mounted for energy calibration during the experiment, see fig. 1. The C-foil was situated nearly parallel to the telescope detector. The telescope consists of a thin proportional gas detector working as a ΔE -detector and a surface barrier silicon detector, in our case with 100mm^2 area and $150\mu\text{m}$ thick. It was crucial to design a gas counter that combined low stopping power and small dead time with acceptable resolution. The demands for a low energy cut-off and small dead time ruled out the classical cylindrical proportional counter with its relatively high pressure and long electron drift times. Instead a hybrid of a parallel-plate counter and a proportional counter was constructed where the charged particles traverse the detector perpendicularly to two parallel wire planes, one tightly wound (wire distance 0.5 mm) connected to ground acting as cathode and the other with wires 2

mm apart connected to positive high voltage. See fig. 1. The planes are separated by 4 mm, yielding a gas-filled charge collection and electron drift volume. In the vicinity of the thin wires in the anode plane a considerable gas amplification takes place. The active volume contains CF_4 [7] with 15 mbar gas pressure and is limited by two thin polypropylene windows. The back window was made electrically conducting by a deposited a 400 Å layer of Al. It was connected to the high voltage to avoid contributions from the passive gas volume behind the HV grid. The charge pulses from the gas detector are fed into an ordinary pre-amplifier and to a spectroscopy amplifier. Even at this very low pressure the detector exhibits an adequate energy resolution to allow charge identification (see fig. 2).

The particles traversing the gas detector were completely stopped in the Si-surface barrier detector. Only the events that gave a signal in both detectors were counted. The solid angle of 0.53% subtended by the telescope detector was determined by the size of the Si-detector. Two more 150mm^2 $700\mu\text{m}$ and 280mm^2 $1000\mu\text{m}$ thick Si-detectors both covered with 0.5 mm thick Al-plates were used to monitor the beta-activity. The solid angles for these detectors were 0.37% and 2.03% of 4π respectively (see figure 1 for details of the set-up). The estimated error in the solid angles was 5%. The relative efficiency of the different detectors was determined by collecting and measuring ^9Li , the β -decay scheme of which is well known [8], under identical conditions.

The energy calibration of the telescope detector was done using the standard α -sources : ^{148}Gd , ^{241}Am and the triple source ^{239}Pu - ^{241}Am - ^{244}Cm . Energy losses were calculated using the parametrization given by Andersen and Ziegler [9]. Measurements of energy losses in the windows and gas were made before and after the experiment. Fixing the thickness of the Al and Au layers to $11\ \mu\text{g}/\text{cm}^2$ and $40\ \mu\text{g}/\text{cm}^2$ respectively we get from the calculated energy losses effective thickness for the polypropylene window and the freon detector of $59\ \mu\text{g}/\text{cm}^2$ and $60\ \mu\text{g}/\text{cm}^2$, respectively.

A final check on the energy calibration of the detector, for reconstruction of the incident particle energy from the events, was done by comparing our measured alpha spectrum from the β -decay of ^8Li to that measured by Wilkinson and Alburger [10] and parametrized in ref. 11.

3.1 Results for ${}^6\text{He}$

A total of 13 hours of beam time was devoted to measuring the β -decay of ${}^6\text{He}$. The deuterons were detected in fast coincidence with a beta particle; events within the time window (106 ns wide) are shown in fig. 3. The deuterons are clearly separated from a beta background. The incident energy was calculated from ΔE and E (correcting also for energy loss in the counter windows). As a check, the theoretical energy loss in the freon gas deduced from the incident energy was compared with the experimental value of ΔE . The difference of the two numbers is plotted in the inset of fig. 3. The two-dimensional spectrum is very clean and the event rate was so low that pile-up was negligible. The number of deuteron events is 362 ± 25 , the number of background events (estimated by taking an equivalent region just above the deuterons) is 10 ± 5 .

To obtain the branching ratio for the deuterons we must know the number of ions deposited in the foil. This can be deduced from the beta count rate in the two solid state detectors present in the set-up. They were both covered with aluminium plates to prevent heavy charged particles from reaching the detectors. Only one of the detectors had sufficiently good signal to noise separation to be used for the normalization. The ratio of geometrical solid angles of the telescope and this detector was measured to be 0.261 ± 0.018 . To check this number we collected ${}^9\text{Li}$ ions during 33 min (from a Ta-foil target with a surface ionization source) with the same set-up after the experiment. The beta-delayed alpha-spectrum from ${}^9\text{Li}$ is well known [8], so we could deduce the total number of decays seen by the telescope from the high energy alpha part. The ratio of this number to the number of betas detected in the monitor Si-detector was 0.289 ± 0.011 ; this number includes both solid angle and efficiency of the two detectors and is in agreement with the determination made above.

Using the latter factor to deduce the total number of ${}^6\text{He}$ decays, we obtain a deuteron branching ratio of $(7.6 \pm 0.6) \cdot 10^{-6}$ for deuterons above our experimental cut-off. This cut-off is at 360 keV but has a width of about 50 keV due to the energy straggling in the detector windows and the gas. Each deuteron is accompanied by an alpha particle (the recoiling daughter nucleus)

that has half the energy of the deuteron. Due to the difference in energy loss of these two particles, none of the events in the selected region could be an alpha particle.

The previous experiment [3] gave a smaller branching ratio, $(2.8 \pm 0.5) \cdot 10^{-6}$ with similar energy cut-off. That experiment was aimed at proving the presence of the beta-delayed deuteron branch by detecting deuteron-alpha coincidences. The solid angles, in that experiment, were necessarily small and several collimators were inserted to suppress the beta particles. The coincidence efficiency of that setup depended quite strongly on the ${}^6\text{He}$ beam size and position on the collection foil, as was also revealed in the Monte Carlo calculations. The present experiment has been aimed at distinguishing deuterons from alphas and has a more reliable set-up. The newly determined lower limit for the branching ratio is therefore more accurate, and we recommend this new value to be used.

Fig. 4 shows the experimental beta-delayed deuteron spectrum. In the first attempts to reproduce this spectrum [3] the R-matrix formalism was used. This assumes a two-step process: ${}^6\text{He}$ decays to states in ${}^6\text{Li}$, that subsequently break up into a deuteron and an alpha particle. The dominating contribution turned out to come from decays through the (virtually excited) ground state of ${}^6\text{Li}$. Although all parameters in the R-matrix expression were known from other experiments, the resulting spectrum turned out to lie more than two orders of magnitude above the experimental points.

A second attempt to explain the data involved beta decays directly into continuum states, i.e. assumed a one-step process. This way of analysis has been pursued in more detailed models [12, 13] the results of which are reproduced in fig. 4. The work of Descouvemont and Leclercq-Willain [12] assumes the two neutrons outside the alpha core in ${}^6\text{He}$ to be quite strongly correlated, but does not attempt to calculate the relative wave function between the two neutrons. Zhukov and collaborators [13] use a more detailed wave function for ${}^6\text{He}$, tested in several other experiments. Both groups use continuum wave functions that fit the experimental d- α phase shift. Note that in both calculations the large distance behaviour of the ${}^6\text{He}$ wave function was important, since the final state wave function is suppressed at close distance due to the Coulomb barrier and the rather small kinetic

energies. The sensitivity to neutron-neutron correlations in ${}^6\text{He}$ was large, so that both groups conclude that the beta-delayed deuteron emission is indeed a sensitive probe of the halo structure. The most realistic calculation [13] is quite close to the experimental points.

None of the calculations mentioned so far reproduces, however, the exact absolute intensity of the experimental spectrum. The wave functions for the mass 6 nuclei are quite well known, so it is unlikely that a quantitatively better agreement could be obtained by improvements in the wave functions. We suggest a mechanism that might explain the low intensities within the approximation of the two-step picture. In the standard R-matrix calculation mentioned above, ${}^6\text{He}$ beta decays to the virtually excited ground state of ${}^6\text{Li}$ which subsequently breaks up. Both of these steps are known to have a large amplitude as the two states are well described by an alpha core plus a di-neutron and a deuteron, respectively. Owing to the strong clustering, one could also imagine decays taking place with the "opposite" ordering, first a break up of ${}^6\text{He}$ into a (virtual) alpha plus di-neutron and then the beta decay of the di-neutron to a deuteron. These decay routes are shown in fig. 5. Two remarks must be made to this suggestion. First, it is not immediately evident that the two decay routes are completely independent; one should of course be careful not to "double-count". Second, both of the routes go through states some MeV off-shell; they are suppressed by several orders of magnitude with respect to the main beta decay of ${}^6\text{He}$ into the ground state of ${}^6\text{Li}$, and it is only because this decay is so simple that we should be able to see the "off-shell" decays (our sensitivity was actually some orders of magnitude better).

We have incorporated this idea in a "toy" model in which the R-matrix expression is changed. The standard expression contains a sum over amplitudes of going through different levels λ in ${}^6\text{Li}$:

$$\left| \sum_{\lambda} \frac{M_{\beta}({}^6\text{He} \rightarrow {}^6\text{Li}_{\lambda}) \gamma({}^6\text{Li}_{\lambda} \rightarrow \alpha + d)}{E - E({}^6\text{Li}_{\lambda})} \right|^2$$

where M_β is the amplitude for the beta decay and γ the amplitude for the particle break up. One would therefore expect the corresponding expression for our two decay routes to be:

$$\left| \frac{M_\beta(^6\text{He} \rightarrow ^6\text{Li}) \gamma(^6\text{Li} \rightarrow \alpha + d)}{E + S_d(^6\text{Li})} + \frac{\gamma(^6\text{He} \rightarrow \alpha + ^2n) M_\beta(^2n \rightarrow d)}{-E - S_{2n}(^6\text{He})} \right|^2$$

The two numerators are here naturally of the same order of magnitude, whereas the two denominators are of the same absolute magnitude but opposite sign (as the virtual states lie on opposite sides of the physical state in the two cases). The two fractions have, furthermore, the same energy dependence so that if a cancellation occurs it would be present in a wide energy interval - this is an unusual feature and very encouraging as the data seem to require this. We know all parameters in the expression except for the product in the second numerator; so we define ξ via:

$$\gamma(^6\text{He} \rightarrow \alpha + ^2n) M_\beta(^2n \rightarrow d) = \xi [M_\beta(^6\text{He} \rightarrow ^6\text{Li}) \gamma(^6\text{Li} \rightarrow \alpha + d)]$$

There is then only one free parameter, and it turns out that both the shape and the intensity of the deuteron energy spectrum can be reproduced for $\xi \approx 0.65$. It would be premature to take this good agreement as proof of the existence of "inverse ordering" in beta-delayed particle emission, but it indicates that similar mechanisms might have to be invoked in order to explain the data.

It is noteworthy that all calculated spectra peaked below our experimental cut-off (see fig. 4). The total branching ratio for deuteron emission will therefore be somewhat larger than our present result. It would be very interesting, but also experimentally difficult, to extend the measurements to lower energies, as this would give more constraints on the theoretical models.

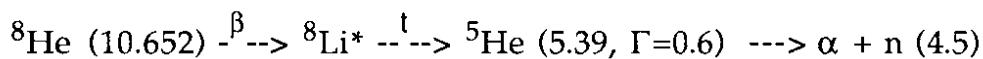
3.2 Results for ^8He

Close to seven hours (400 min) were spent measuring the charged particles emitted in the beta-decay of ^8He . A total of 7938 ± 120 triton events were detected. The event selection was done following the same method as

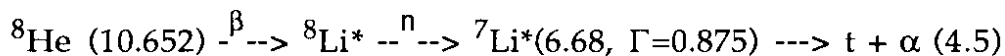
for ${}^6\text{He}$ except for two extra corrections, namely a background in the ΔE - E plot from alpha particles and a tail at low energies from beta particles.

The response function of the Si E-detector has a low energy tail due to scattering of particles from the surroundings into the detector and incomplete charge collection. From the ${}^{148}\text{Gd}$ and ${}^{241}\text{Am}$ calibration sources this tail was found to be approximately flat and to contain 3% and 4% of the total intensity for 3.2 MeV and 5.5 MeV, respectively. As the energy loss decreases for high particle energies the most energetic alpha particles can have the same energy loss, ΔE , as some of the tritons. The tail from such alphas in the E-detector gives a small background for the true triton events. The beta particles give an exponentially falling distribution in the E-detector and can be safely estimated and subtracted from the final spectrum.

Essentially all alpha particles originated in the beta decay of ${}^8\text{Li}$ fed in the ${}^8\text{He}$ decay via the 84% beta branch [14] to the 0.985 MeV level. The only other possibility of producing alphas occurs in the triton emission in the two energetically allowed branches



and



both giving p-wave tritons. The energies in MeV are taken from ref. 15. In the first branch, the alpha spectrum peaks at 300 keV, below the telescope cut off. Only 22% of the intensity of this spectrum could be detected by the telescope corresponding to a 0.2% of the total number of alphas. In the second branch they would have 3/4 of the triton energy, but as we shall demonstrate later the maximum contribution to the branch is only about 2 %. We can therefore safely put the triton branching ratio on an absolute scale. The result is $(8.0 \pm 0.5) \cdot 10^{-3}$, in good agreement with the previous experiment [16].

Fig. 6 shows the triton energy spectrum. The events are added into 25 keV bins and plotted in the center of the bin. The new triton spectrum differs somewhat from the previous one [16] for the following reasons: a more extensive energy calibration was done including, in particular, the comparison with alpha particles from the ${}^8\text{Li}$ decay [11]. A more careful

analysis of the energy losses in the dead layer was also made. We follow ref. 4 in using R-matrix theory to fit the spectrum, but we have made several simplifying assumptions. First, shell model calculations [5,17] predict the existence of four 1^+ levels in ${}^8\text{Li}$ within the Q-window of ${}^8\text{He}$. There is independent experimental evidence of two 1^+ levels at 0.985 MeV and 3.21 MeV and a third was postulated in ref. 14 to fit the beta delayed neutron spectrum. None of these levels could contribute strongly to the triton branch, so we shall assume that the tritons come from the fourth level and use a single level approximation. Furthermore, for simplicity, we use the single channel approximation. This turns out to be sufficient for describing the triton spectrum alone.

In the calculations, the widths of the particle emitting levels and the recoil of the (triton emitting) ${}^7\text{Li}$ nucleus for the second of the branches listed above have to be included. In this branch, the triton spectrum is mainly determined by the properties of the intermediate level in ${}^7\text{Li}$. As the triton spectrum peaks around 1.2 MeV the level must be situated around 4 MeV if the second branch alone should fit the data. The only candidate in ${}^7\text{Li}$ is the level at 4.63 MeV ($\Gamma=0.093$ MeV, $J^\pi=7/2^-$), but as argued earlier [14] the contribution from this level is likely to be small as the neutrons would have to be emitted as an f-wave. This is not likely to be the dominating decay channel for the level in ${}^8\text{Li}$. The calculated triton spectrum also appears quite different in shape from the experimentally measured one. Our fit will therefore make use of the first branch only; the energy and width of the intermediate level in ${}^8\text{Li}$ are here directly reflected in the shape of the triton spectrum. The final formula we use can be found in appendix A, p. 209 of ref. 8. It contains four free parameters: an overall normalization factor, the energy and reduced width of the excited state in ${}^8\text{Li}$ and the radius for the triton channel (the channel radius for the subsequent neutron emission was fixed at 3 fm). A chi-square minimization resulted in an energy of 9.3 ± 0.1 MeV, $\gamma = 0.978 \pm 0.012$ MeV $^{1/2}$ and a channel radius of 3.7 fm, the corresponding theoretical spectrum is shown in fig. 6 as a solid line. Changing the channel radius for the neutron from 3 fm to 4 fm give values for the energy and the reduced width that agree within the error bars. There seems to be no need to introduce either the second decay branch, or other levels in ${}^8\text{Li}$. From the high energy part of the triton spectrum we get a maximum relative contribution of the second branch of 2 %.

We should stress that this fit, although very good, might not be the only way of explaining the data. Decays directly to the continuum might also take place for ${}^8\text{He}$, and the situation for ${}^6\text{He}$ should be taken as a warning against hastened conclusions. However, we see no immediate need to invoke other explanations than the present one.

In order to deduce the total feeding to the 9.3 MeV level in ${}^8\text{Li}$ we must also examine whether channels other than triton emission could noticeably contribute to its deexcitation. The Wigner reduced width for this level to the $t + {}^5\text{He}$ branch is $1.9 \text{ MeV}^{1/2}$ which is larger than the level found in our fit, showing no need for other channels to be present. The only other open channels are neutron emission to the ground state ($E = 2.033, J^\pi = 3/2^-$) and first excited state ($E = 0.4776 \text{ MeV}, J^\pi = 1/2^-$) of ${}^7\text{Li}$. These give high energy neutrons, up to 8 MeV, that are hard to detect directly experimentally. We can, however, look for the corresponding recoiling ${}^7\text{Li}$ nuclei. Our energy loss calculations give an efficiency in the telescope of 93% for Li ions of energy 500 keV and reaches 100% efficiency at 680 keV. A neutron branch from the 9.3 MeV level would give 26% of the recoil ions above 500 keV; such events would be merged with the alpha particles in the ΔE - E spectrum in figure 2 and correspond to alphas of energy up to 1 MeV. We have compared our alpha spectrum with the one listed in ref. 11, and we have a deviation at low energies that might be due to the ${}^7\text{Li}$ recoil ions, but the uncertainties are too large to allow firm conclusions to be drawn. It should also be noted that the alpha spectrum below 800 keV has not been reliably measured, but must be taken from the theoretical fit. We assume for the moment that the main decay channel of the 9.3 MeV level in ${}^8\text{Li}$ proceeds via triton emission, and obtain a $B(\text{GT})$ of 5.18, corresponding to a $\log(ft)=2.87$. If other channels were present this would be a lower limit, only. We note that this is among the largest $B(\text{GT})$ values observed confirming the superallowed nature of this transition [18].

We note for completeness that a beta delayed deuteron branch would give deuterons of a maximum energy of 580 keV. They could not have been resolved in the present experiment.

4. Summary and Outlook

We have measured the beta delayed charged particle branches from the decays of ${}^6\text{He}$ and ${}^8\text{He}$ with the use of a telescope detector specially designed to identify low energy charged particles of different charges. These branches are expected to be particularly sensitive to neutron halos or similar structures. It has recently been suggested [19] that both nuclei have a thick neutron skin around an alpha core. This results of an analysis of interaction and neutron removal cross sections of high energy radioactive beams.

The beta delayed deuteron branch from ${}^6\text{He}$ was confirmed with a revised lower limit for the branching ratio of $(7.6 \pm 0.6) \cdot 10^{-6}$. The deuteron spectrum has a smooth shape which is mainly dominated by phase space and penetrability factors. The shape is therefore fairly well reproduced by the different calculations shown in fig. 4, but the absolute intensity of the spectrum could not be reproduced in a conventional R-matrix calculation or in calculations assuming the direct decay to the continuum to be dominant although the latter came much closer. We have suggested a new mechanism to be present, namely decays where the particle emission (through a virtual state) precedes the beta decay. Such a mechanism clearly relies on the large overlap of ${}^6\text{He}$ with an alpha particle and a "di-neutron".

The beta delayed triton branch from ${}^8\text{He}$ was remeasured, and agreed with the previous measurement. The triton branching ratio was determined to be $(8.0 \pm 0.5) \cdot 10^{-3}$. The present spectrum is well fitted by a R-Matrix calculation using a single 1^+ level in ${}^8\text{Li}$ at 9.3 MeV, the energy and reduced width of this level could be deduced with good accuracy from the data. The reduced width for triton emission is, as already noted in ref. 4, several times larger than expected from shell model calculations. This might indicate that strong three nucleon correlations are present in the excited level. The high B(GT) value implies a large overlap between the wave function of the 9.3 MeV state in ${}^8\text{Li}$ and the ground state of ${}^8\text{He}$. It is thus tempting to conclude that there are sizeable correlations between - most likely - all four "outer" neutrons in ${}^8\text{He}$ [20].

In conclusion, we have presented experimental evidence for anomalies in the beta decays of both ${}^6\text{He}$ and ${}^8\text{He}$: the astonishingly small branching ratio for deuterons in ${}^6\text{He}$ and the surprisingly large one for tritons in ${}^8\text{He}$.

We have suggested that the explanation might in both cases be sought in the special structure of these nuclei; both have a well defined core, the alpha particle, surrounded by fairly loosely bound neutrons.

Acknowledgements

We would like to thank P.G.Hansen and M.V.Zhukov for discussions.

References

1. I. Tanihata, H. Hamagaki, O. Hashimoto, Y. Shida, N. Yoshikawa, K. Sugimoto, O. Yamakawa, T. Kobayashi, N. Takahashi, *Phys. Rev. Lett.* **55** (1985) 2676
2. P.G. Hansen, "Nuclear structure at the drip lines" Int. Nuclear Physics Conf., Wiesbaden 1992 , to be published in *Nucl. Phys. A*
3. K. Riisager, M.J.G. Borge, H. Gabelmann, P.G. Hansen, L. Johannsen, B. Jonson, W. Kurcewicz, G. Nyman, A. Richter, O. Tengblad, K. Wilhelmsen, *Phys. Lett.* **B235** (1990) 30
4. F.C. Barker and E.K. Warburton, *Nucl. Phys.* **A487** (1988) 269
5. N. Kumar, *Nucl. Phys.* **A225** (1974) 221
6. J.P. Biersack and L.G. Haggmark, *Nucl. Instrum. Methods* **174** (1980) 257-269
7. J.D. Robertson, Nuclear Science Divison, Lawrence Berkeley Laboratory, private communication
8. G. Nyman, R.E. Azuma, P.G. Hansen, B. Jonson, P.O. Larsson, S. Mattsson, A. Richter, K. Riisager, O. Tengblad, K. Wilhelmsen, *Nucl. Phys.* **A510** (1990) 189
9. H.H. Andersen and J.F. Ziegler, *The stopping and ranges of ions in matter*, vol. 3,4 (Pergamon, New York 1977)
10. D.H. Wilkinson and D.E. Alburger, *Phys. Rev. Lett.* **26** (1971) 1127
11. F.C. Barker, *Aust. J. Phys.* **42** (1989)25
12. P. Descouvemont and C. Leclercq-Willain, *J. Phys.* **G18** (1992) L99
13. M.V. Zhukov, B.V. Danilin, L.V. Grigorenko, N.B. Shul'gina, preprint NORDITA 92/79 N (1992), submitted to *Phys. Lett.*

14. T. Björnstad, H.Å. Gustafsson, B. Jonson, P.O. Larsson, V. Lindfors, S. Mattsson, G. Nyman, A.M. Poskanzer, H.L. Ravn, D. Schardt, Nucl. Phys. **A366** (1981) 461
15. F. Ajzenberg-Selove, Nucl. Phys. **A413** (1984) 1
16. M.J.G. Borge, M. Epherre-Rey-Campagnolle, D. Guillemaud-Mueller, B. Jonson, M. Langevin, G. Nyman, C. Thibault, Nucl. Phys. **A460** (1986) 373
17. H.D. Knox, D.A. Resler, R.O. Lane, Nucl. Phys. **A466** (1987) 245
18. M.J.G. Borge, P.G. Hansen, L. Johannsen, B. Jonson, T. Nilsson, G. Nyman, A. Richter, K. Riisager, O. Tengblad, K. Wilhelmsen, Z. Phys. **A340** (1991) 255
19. I. Tanihata, D. Hirata, T. Kobayashi, S. Shimoura, K. Sugimoto, H. Toki, Phys. Lett. **B289** (1992) 261
20. K. Riisager, M.J.G. Borge, H. Gabelmann, P.G. Hansen, L. Johannsen, B. Jonson, W. Kurcewicz, G. Nyman, A. Richter, O. Tengblad, K. Wilhelmsen, Proc. Workshop on Nuclear Structure of Light nuclei far from Stability Experiment and theory, Obernai 1989, ed. G. Klotz (Centre de Recherches Nucleaires, Strasbourg, 1991) p 267

Figure Captions

Figure 1. Schematic picture of the experimental set up. The collimated radioactive ion beam was stopped in a C-foil mounted on a wheel. Opposite the C-foil a ^{148}Gd source was placed to facilitate energy calibration during the experiment. A ΔE -E telescope detector consisting of a thin proportional gas (CF_4) detector (ΔE) and a Si surface barrier detector was used to detect the emitted charged particles. Two other Si-detectors covered with Al-plate were used to monitor the beta activity. For details about the detectors see text.

Figure 2. ΔE plotted as a function of E for β -delayed charged particles from ^8He . The spectrum corresponds to 30 min of collection. Note the low energy losses in the freon gas. The inset shows the comparison of the experimental energy loss in the gas detector with the theoretical loss deduced from the incident energy assigned to the tritons. The histogram includes all triton events.

Figure 3. Two dimensional ΔE -E diagram of charged particles associated with the ^6He β -decay: the betas are well separated from the deuteron events. Comparison, for all deuteron events, between the energy loss in freon and the theoretical value is shown in the inset.

Figure 4. Deuteron spectrum from the ^6He β -decay. The points are the experimental data given in the center of a 40 keV bin in the laboratory system. The vertical scale given in counts/bin can be converted into intensity per second and per MeV by the factor $4.0 \cdot 10^{-7}$. The dotted line [12] and the dashed line [13] correspond to calculations considering break up to the continuum. The solid curve is the result of an extended R-matrix calculation for which a schematic diagram is shown in fig. 5.

Figure 5. Alternative decay routes for the deuterons emitted in the beta decay of ^6He . The dashed lines correspond to the virtual levels through which the decay occurs. The double arrows show how much the levels are off-shell. The final state center of mass energy is E. In the standard route the β -decay happens first. In the other route ^6He breaks up into an alpha and a di-neutron (with center of mass kinetic energy E) which then β -decays.

Figure 6. The experimental and calculated triton energy spectrum from the decay of ^8He . The experimental points are given in the center of a 25 keV bin and are shown with their statistical errors. The continuous line show the theoretical fit to the experimental spectrum in the frame of R-matrix theory. We deduce the energy (9.3 ± 0.1 MeV) and reduced width (0.978 ± 0.012 MeV $^{1/2}$) of the excited level in ^8Li from the fit. The arrow shows the lower energy limit for the reliable triton events.

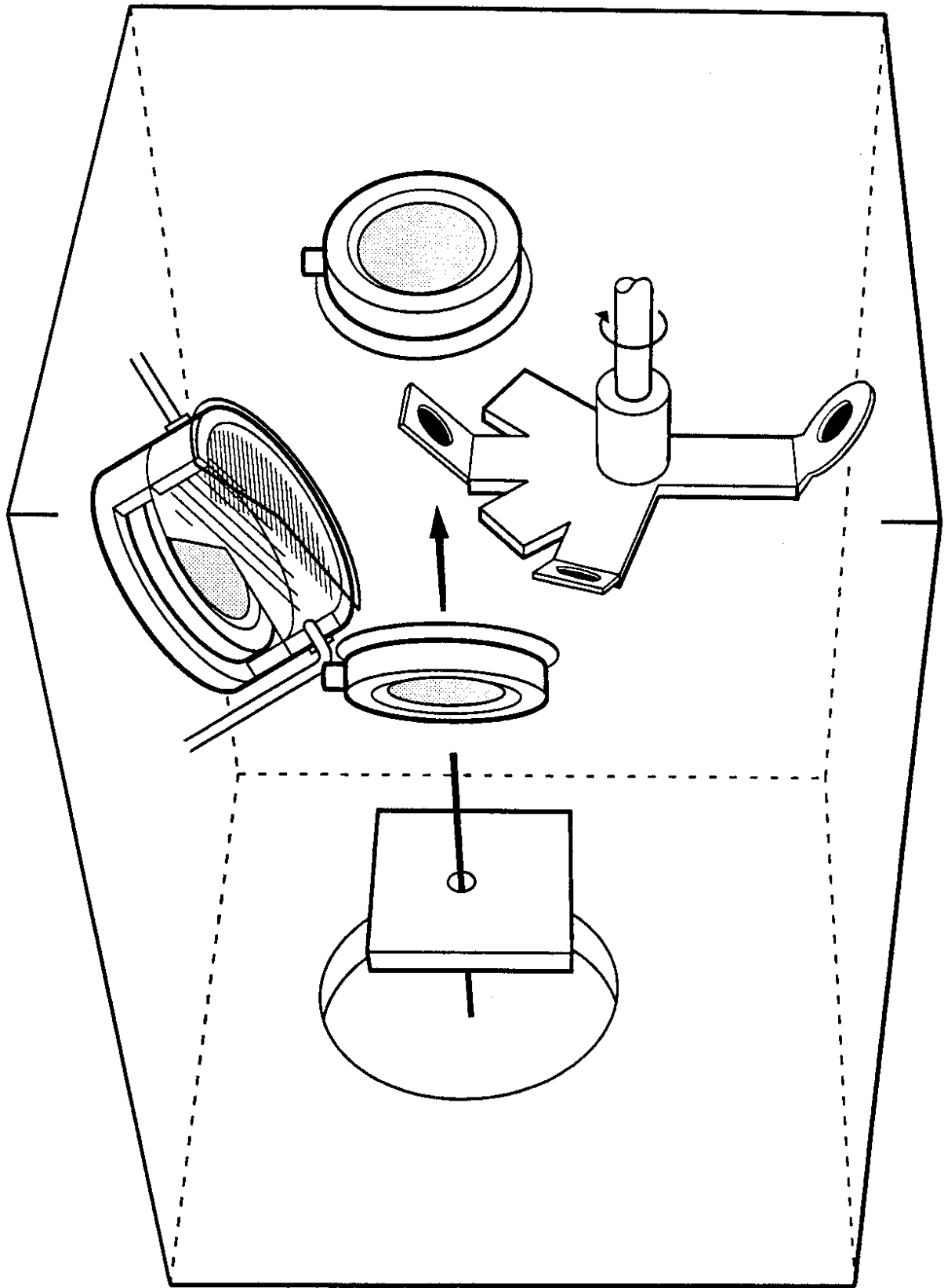


Fig. 1

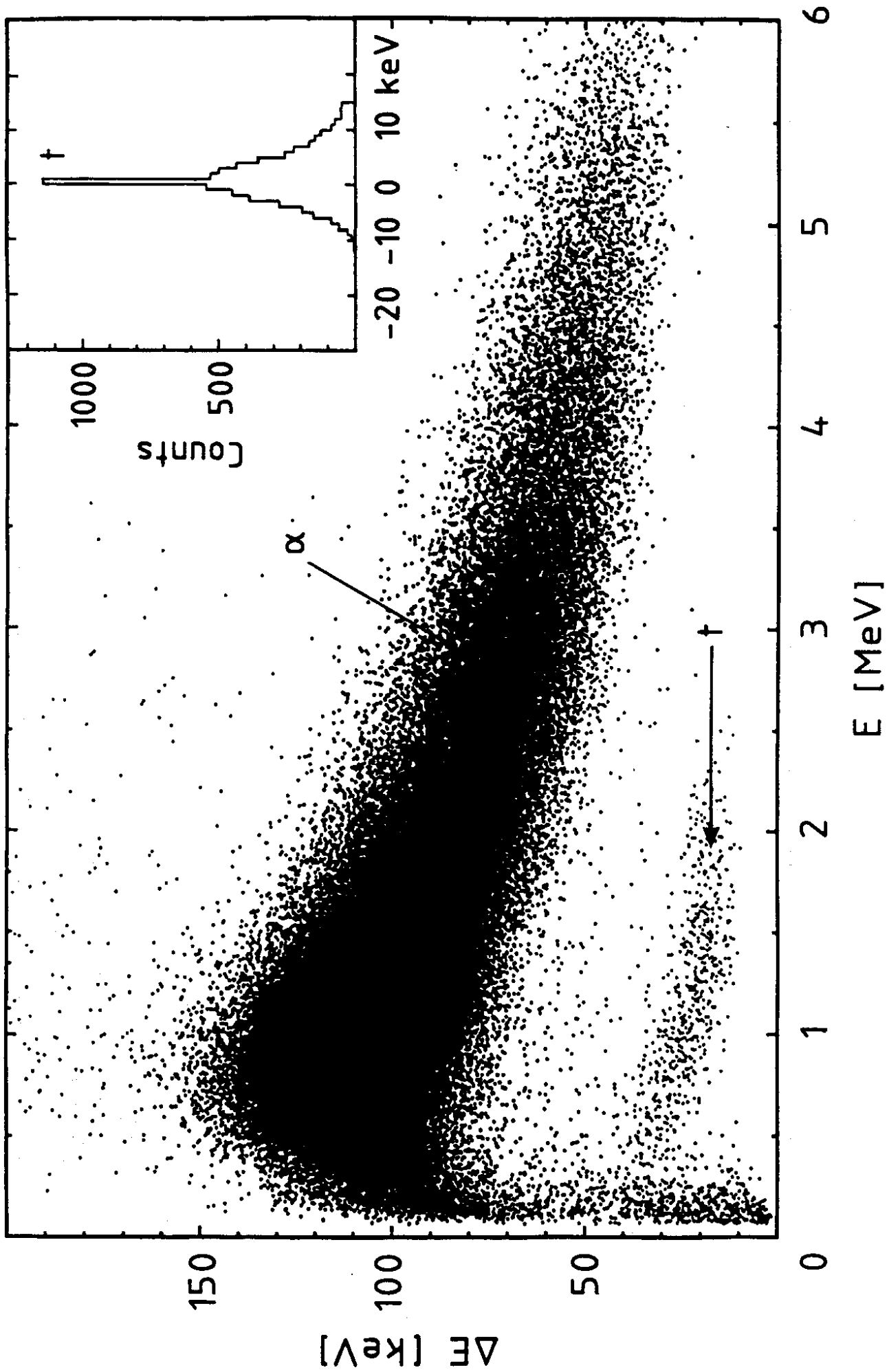


Fig. 2

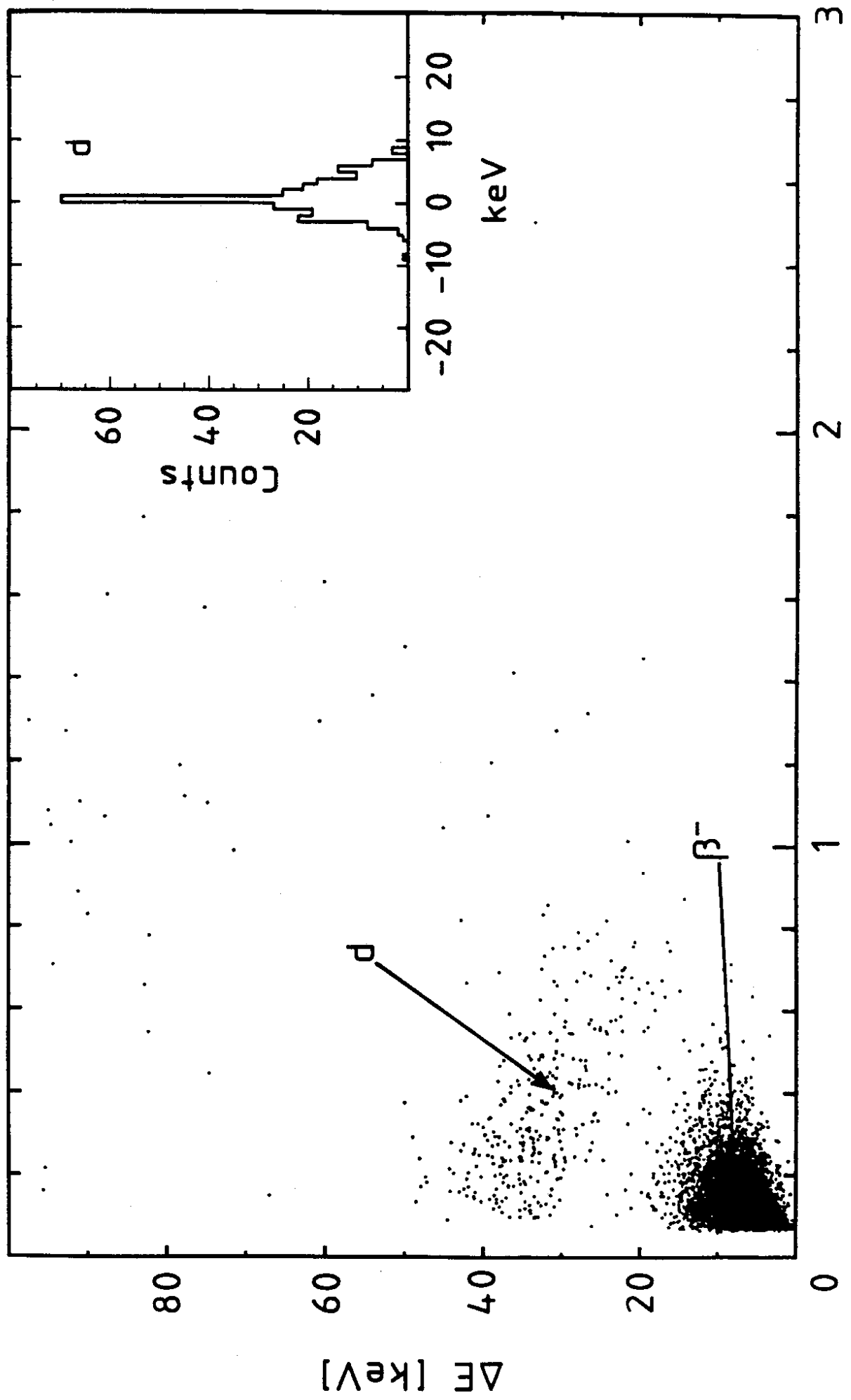


Fig. 3

E [MeV]

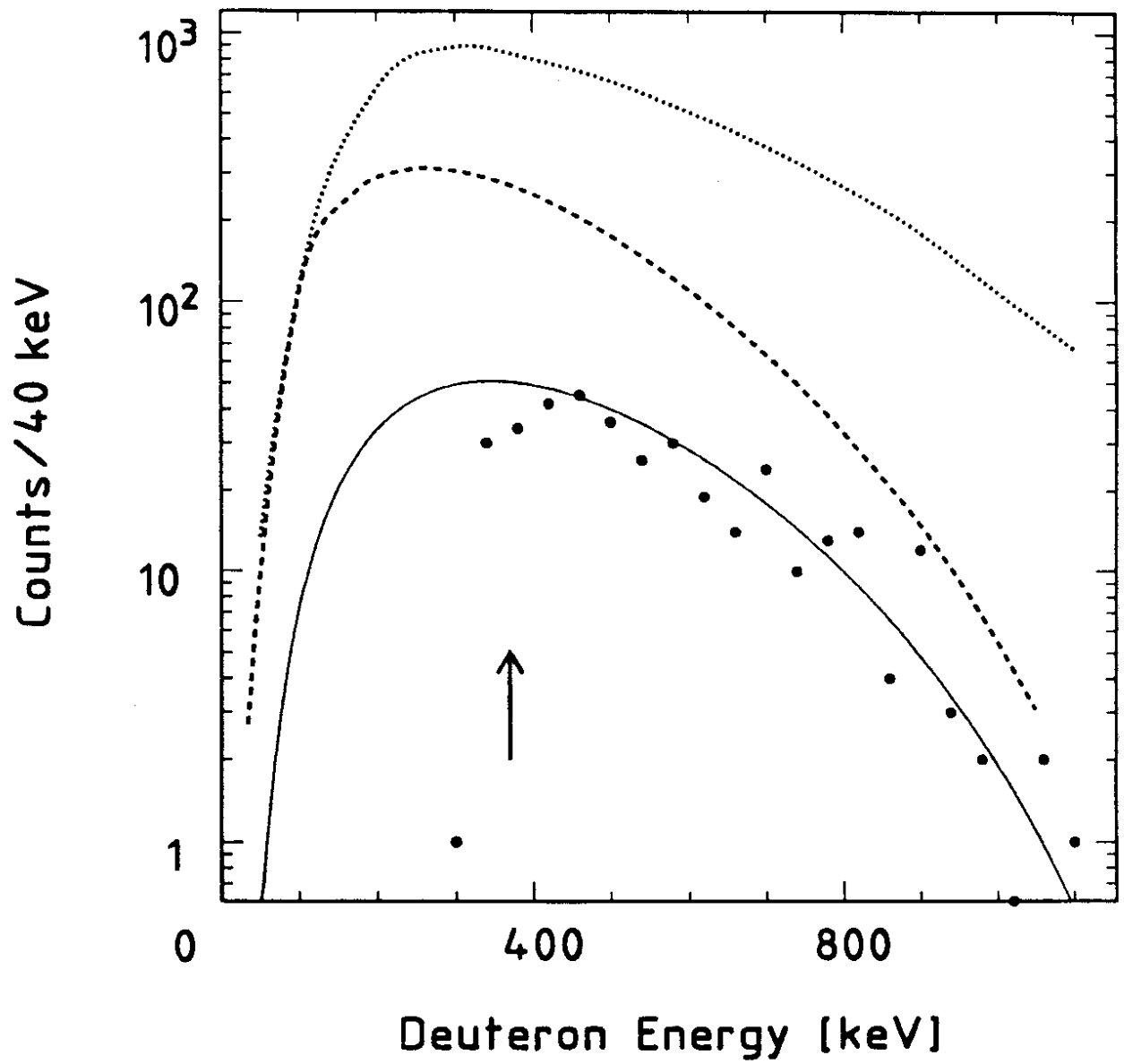


Fig. 4

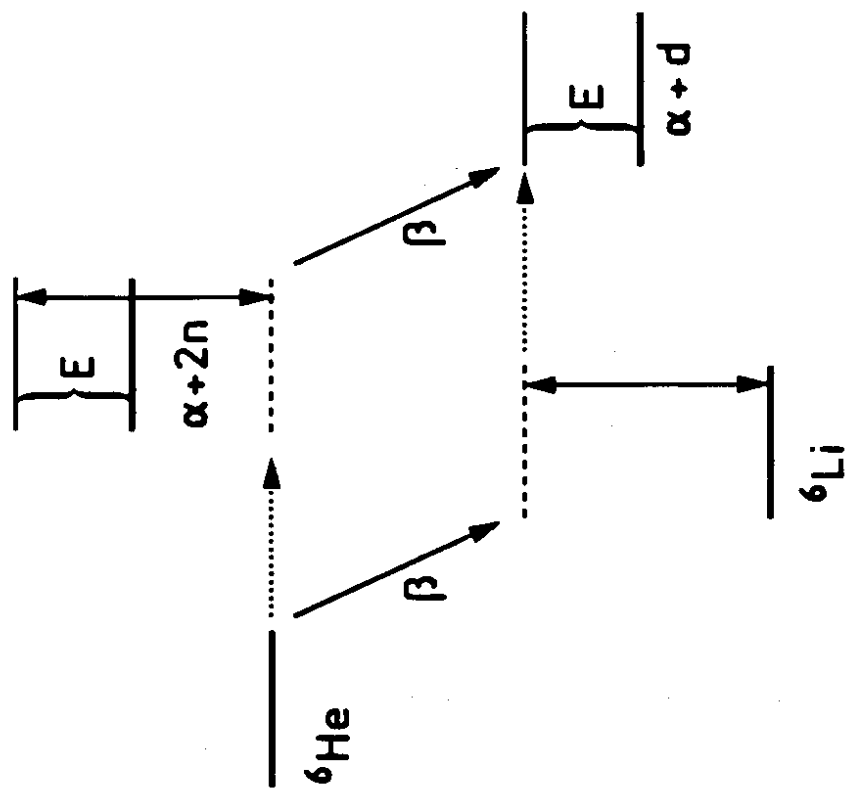


Fig. 5

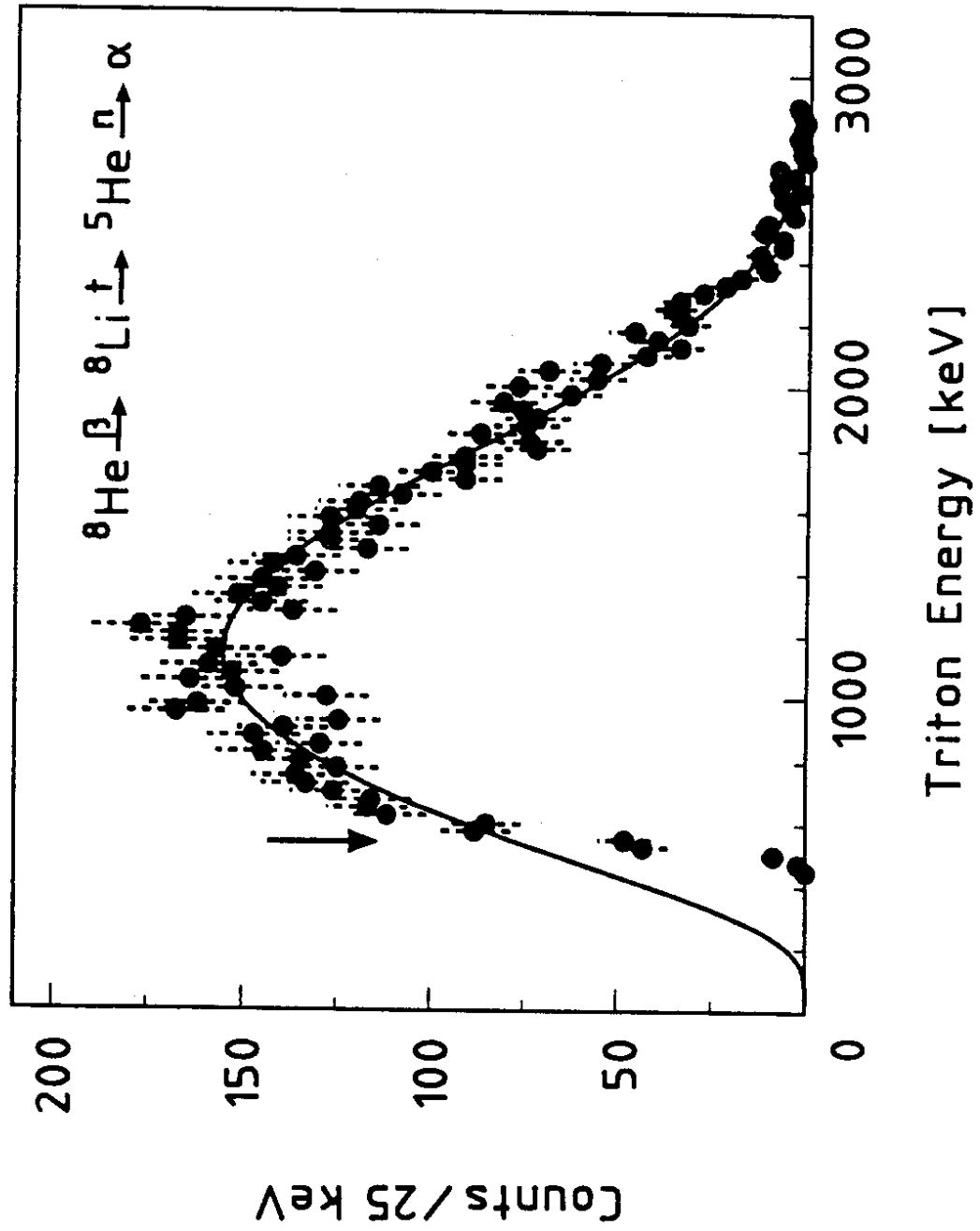


Fig. 6